Chaos and order in ion traps and storage rings

Reinhold Blümel

Fakultät für Physik, Albert-Ludwigs-Universität,
Hermann-Herder-Str. 3, D-79104 Freiburg, Germany

Abstract. Chaos and order play a major role in the physics of Coulomb crystallization in traps and storage rings. This fact is illustrated with the help of the following four topics: (i) fractional frequency parametric resonances in a Paul trap, (ii) the chaos scenario in the dynamic Kingdon trap, (iii) beam crystallization criteria and (iv) suppression of synchrotron radiation by crystallized beams.

I. PARAMETRIC RESONANCE IN A PAUL TRAP

The equations of motion of a single charged particle in a Paul trap can be reduced to three decoupled Mathieu equations of the type (see, e.g., [1])

$$\ddot{x} + [a - 2q\cos(2t)]x = 0, \tag{1}$$

where a and q are control parameters. The parameter space $\mathcal{P}$ of (1) is two dimensional. For a given point $(q, a) \in \mathcal{P}$ the solution $x(t)$ of (1) may either be stable or unstable. Thus we can decompose $\mathcal{P}$ into regions that correspond to stable and unstable solutions of (1), respectively. For the range $0 \leq q \leq 1$, $0 \leq a \leq 10$, the decomposition of $\mathcal{P}$ is shown in Fig. 1. The white regions correspond to stable solutions of (1), the black regions to unstable solutions. The unstable regions form tongues that touch the a axis at $a = \quad n^2$, $n = 1, 2, \ldots$. The black regions in Fig. 1 are called regions of parametric instability.

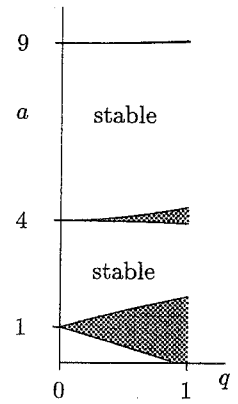

FIGURE 1. Stable (white) and unstable (black) regions of the parameter space $\mathcal{P} = \{(a, q)\}$ of the Mathieu equation.

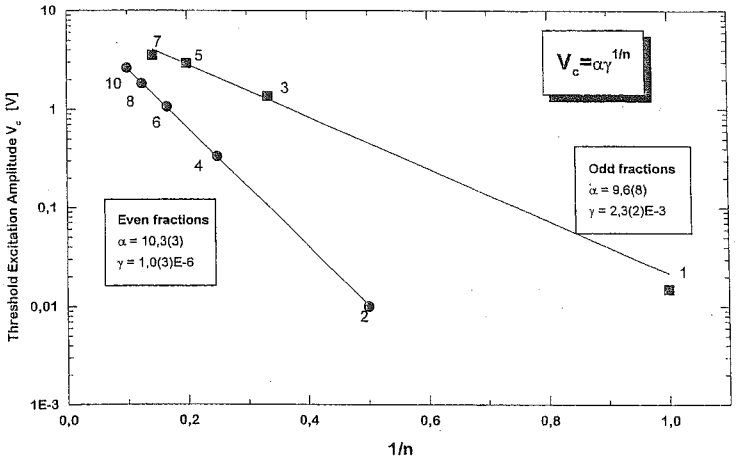

FIGURE 2. Measured critical voltages vs. $1/n$ show odd-even staggering.

Knowledge of the stable and unstable regions of $\mathcal{P}$ is useful for analyzing a recent experiment [2] on the parametric excitation of a large uncooled cloud of N_2^+ ions stored in a Paul trap. In this experiment a weak excitation voltage (on the order of 100 mV to a few Volts, frequency ω) is applied to the end caps of the trap in addition to the trap voltage (on the order of 100 V, frequency $\Omega \approx 2\pi \times 3$ MHz). Denoting by ω_z the axial secular frequeny of the center-of-mass motion of the ion cloud, the experiment detected very efficient excitation of the stored ions accompanied by a large particle loss at excitation frequencies $\omega_n \approx 2\omega_z/n$, $n = 1, 2, \ldots$.

The simplest model for describing the axial motion of the ion cloud retains only its center-of-mass coordinate Z and uses the pseudopotential approximation [3]. The equation of motion reads

$$\ddot{Z} + \omega_z^2 Z = F\cos(\omega t)Z, \tag{2}$$

where F is the strength of the additionally applied excitation field. The substitution $\tau = \omega t/2$ turns (2) into a Mathieu equation of the type (1) with $a = (2\omega_z/\omega)^2$. Since, as mentioned above, the Mathieu equation is unstable in the vicinity of $a_n = n^2$, the solutions of (2) are unstable for $\omega_n = 2\omega_z/n$ as observed in the experiments.

Since the instability tongues of Fig. 1 touch the a axis, the simple equation (2) predicts that for any nonzero value of F (F not too large) there is an ω in the vicinity of ω_n, such that 100% particle loss occurs. But this is not what is observed in the experiments. Experimentally there is a measurable particle loss only if F exceeds a critical excitation strength F_n. In order to understand this, we add a damping term to (2). This is because it is known from the theory of the damped Mathieu equation that in the presence of damping the instability tongues shown in Fig. 1 move away from the a axis, resulting in a contiguous region in the vicinity of the a axis where the fixed point $Z = 0$ of (2) is stable. Thus damping is a possible mechanism for explaining the existence of a critical excitation strength. Adding a damping term to (2) followed by appropriate scaling results in [2]

$$\ddot{Z} + \gamma\dot{Z} + Z = f\cos(\nu\tau)Z. \tag{3}$$

Here γ is the damping constant, f is the scaled excitation strength, ν is the scaled excitation frequency, τ is the scaled time and the dot refers to differentiation with respect to τ. According to a formula stated without derivation in Landau and Lifshitz [4] the critical excitation strength f_n at $\nu_n = 2/n$ is given by

$$f_n = \alpha_n(\gamma)\,\gamma^{1/n}. \tag{4}$$

We checked in various representative cases that $\alpha_n(\gamma)$ depends only weakly on n and γ. Thus plotting the logarithms of the measured critical excitation voltages versus $1/n$ should result in a collection of data points that essentially fall onto a single straight line with a shift that is associated with α and a slope given by $\log(\gamma)$. Figure 2 shows the experimental result. Instead of the expected single line the data points fall onto two different straight lines corresponding to even and odd n, respectively. This effect was called "odd-even staggering" in [2]. The reason for this effect is currently not known.

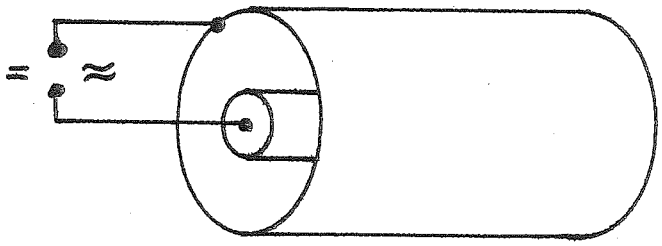

FIGURE 3. Sketch of the cylindrical dynamic Kingdon trap.

II. CHAOS SCENARIO IN THE DYNAMIC KINGDON TRAP

The cylindrical version of the dynamic Kingdon trap is shown in Fig. 3. It consists of a cylinder capacitor with a superposition of an ac voltage $V_{\rm ac}$ and a dc voltage $V_{\rm dc}$ applied between the inner and the outer cylinder of the trap. This trap was developed by E. Teloy at Freiburg University in the 1960s. It was subsequently investigated analytically, numerically and experimentally in the framework of two student theses [5,6]. In contrast to the Paul trap which relies on oscillating quadrupole fields, the dynamic Kingdon trap relies on a superposition of static and dynamic monopole fields. There are various versions of this trap. The early Freiburg trap used an axially symmetric design [5,6]. A radially symmetric version of the dynamic Kingdon trap was recently investigated experimentally [7].

In contrast to the single particle Paul trap which is completely integrable, the dynamic Kingdon trap exhibits chaos and a period doubling scenario even in the case of a single trapped particle [8–12]. It can be shown [12] that in the presence of damping the equation of motion of the radial coordinate x of a charged particle stored in a dynamic Kingdon trap can be cast into the form of a nonlinear damped Mathieu equation

$$\ddot{x} \; + \; \gamma\dot{x} \; + [1 - 2\eta \, \cos(2t)] \, x^{\alpha} \; = \; 0, \tag{5}$$

where γ is the damping constant, $\eta \sim V_{\rm ac}/V_{\rm dc}$ is the control parameter and α is the nonlinearity exponent. For the cylindrical trap $\alpha = -1$; for the radially symmetric trap $\alpha = -2$. Both types of traps exhibit a mixed phase space with regular and chaotic regions. In the following we focus on the cylindrical trap. For $\gamma = 0$ (the Hamiltonian case) a phase-space portrait of the cylindrical trap is shown in Fig. 4 (a) for $\eta = 4$. The fixed point at $(x, \dot{x}) \approx (2.2, 0)$

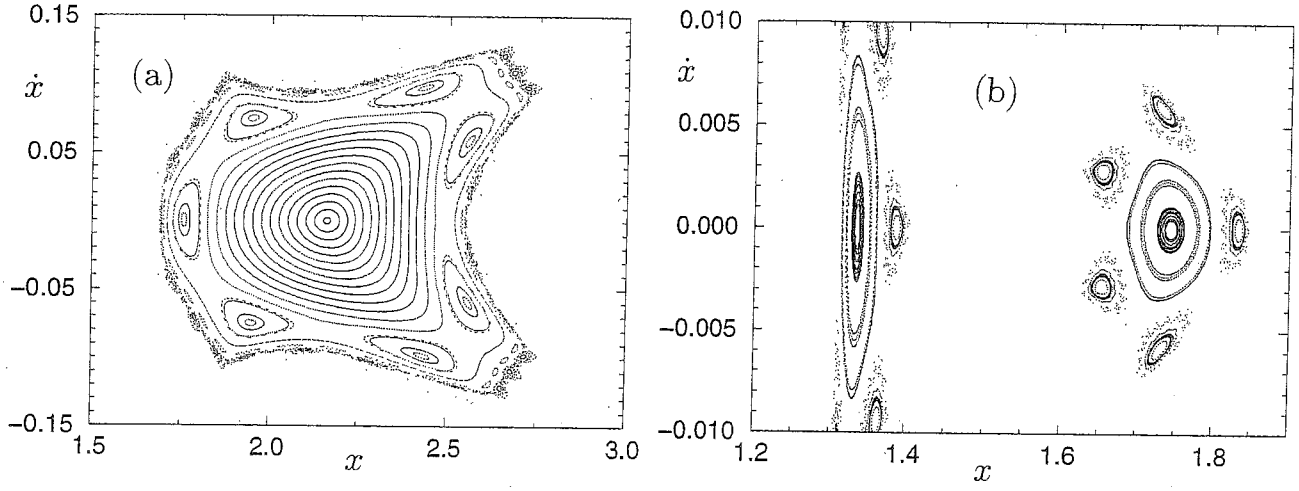

FIGURE 4. Phase-space portrait of the cylindrical dynamic Kingdon trap in the vicinity of the primary fixed point. (a) $\eta = 4$, (b) $\eta = 3.05$.

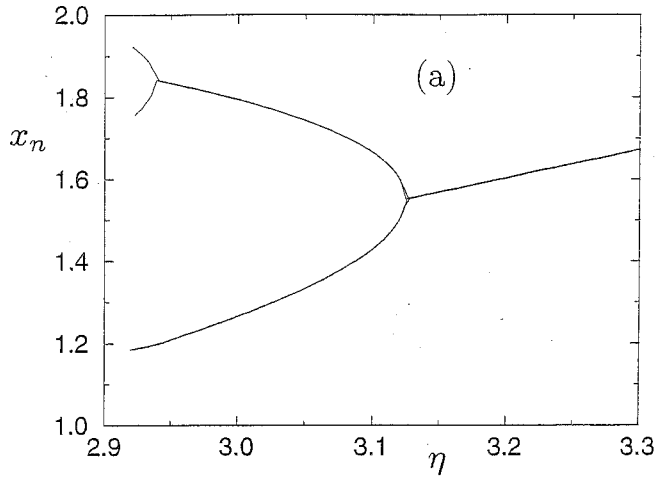

FIGURE 5. Bifurcation diagram of the cylindrical dynamic Kingdon trap.

corresponds to the main trapping region of the dynamic Kingdon trap. It is surrounded by island chains and chaotic regions. Decreasing the value of the control parameter η, the main fixed point in Fig. 4 (a) exhibits a series of bifurcations at well defined values η_n, $n = 1, 2, ...$ of the control parameter η. The first few η_n values are given by $\eta_1 \approx 3.125$, $\eta_2 \approx 2.938$, $\eta_3 \approx 2.917$ and $\eta_4 \approx 2.915$. At $\eta = \eta_1$ the central island in Fig. 4 (a) splits into two. The resultig situation immediately after the bifurcation is shown in Fig. 4 (b). Each of the two resulting islands splits again at $\eta = \eta_2$.

The bifurcation scenario of the main fixed point of the dynamic Kingdon trap is shown in Fig. 5. It reminds of the bifurcation diagram of the logistic mapping [10]. The bifurcation diagram shows the position of the stable islands of the dynamic Kingdon trap as a function of η. With the help of a Fourier analysis an approximate analytical value for the position η_1 of the first bifurcation was recently computed [12]. It is given by $\eta_1 \approx (15 + \sqrt{485})/12 \approx 3.085$ and is in good agreement with the numerical value.

III. DIAGNOSTIC METHOD FOR BEAM CRYSTALLIZATION

Crystallization of a large number of ions in a circular model storage ring was recently demonstrated [13]. Because of their near-relativistic speeds, however, crystallization of heavy ions in large-scale storage rings is much harder to achieve. Several laboratories are currently working on this problem [14]. But even if a crystallized beam is actually present in a storage ring, there remains the question of how to prove it. For the relatively slow ions in traps and model storage rings this problem has been solved more than a decade ago using direct optical imaging [15,16]. In the case of fast beams, however, this method does not work and one has to resort to more indirect diagnostic methods. One of these methods is to pick up the Schottky noise of the beam. But this method, as implemented in current storage rings, is mainly sensitive to the longitudinal characteristics of the ion beam. Indeed, longitudinal ordering has already been inferred this way [17]. Another indirect method was proposed recently [18,19]: Absence of heating of a crystalline beam. This method is based on the mixed nature of phase space with its regular and chaotic regions (see, e.g., Fig. 4). The crystalline phase of a beam in a storage ring corresponds to a fixed point of phase space. In the case of a simple geometric structure of the beam, such as e.g. a linear chain of ions, this fixed point corresponds to a stable island. It is surrounded by a chaotic sea. If an ion beam in a storage ring is just cold, but not yet crystallized, its phase-space trajectory explores the chaotic sea. Without a cooling mechanism the beam's thermal energy increases due to chaotic diffusion. But if the beam is cold enough, it enters the stability region of the fixed point and no heating occurs even in the absence of a cooling mechanism. Thus, in order to prove that the beam in a storage ring is crystallized, the following three steps may be followed:

1) The cooling devices are switched on. The beam reaches a final cold state whose nature (crystallized or not) is to be determined.
2) All the cooling devices are switched off.
3) Evaluation: (i) If the beam heats up immediately following the shut-down of the cooling devices, the beam

was cold, but not crystallized. (ii) If the beam's temperature does not change following the shut-down of the cooling devices, the beam was crystallized.

The validity of this criterion was established with the help of detailed molecular dynamics simulations [19].

IV. SYNCHROTRON RADIATION OF CRYSTALLIZED BEAMS

All the early atomic models based on classical mechanics suffered from a serious shortcoming: the circulating charges, undergoing accelerated motion, continuously radiated energy eventually resulting in the collapse of the atom. In this respect Thomson's raisin cake model [20] was no exception. But Thomson hit upon a brilliant idea to save his model: suppression of electromagnetic radiation due to Coulomb crystallization [21]. For the six electrons of the carbon atom, e.g., arranged equi-spaced on a ring, he computed a suppression factor of $\approx 10^{-17}$ [21]. Thus Thomson may have been the first to dicuss suppression of radiation by geometrically ordered charges.

Nowadays geometrically ordered charges are of topical interest again in connection with crystallized beams. Here Thomson's idea of suppression of electromagnetic radiation of ordered accelerated charges leads to the suppression of synchrotron radiation emitted by a crystallized beam [22]. This effect may be used in two different ways: (i) for the development of new electron accelerator schemes and (ii) as a further indirect diagnostic criterion for beam crystallization. Concerning (i), the idea is to cool the electron beam in a cyclic electron accelerator sufficiently such that the energy loss from synchrotron radiation is no longer a serious limitation of the maximal reachable energy of the accelerator. Concerning (ii), a sharp drop in the power of the emitted synchrotron radiation indicates beam crystallization.

ACKNOWLEDGMENTS

The author gratefully acknowledges financial support by the Deutsche Forschungsgemeinschaft (SFB 276).

REFERENCES

1. Ghosh, P. K., *Ion Traps*, Oxford: Clarendon Press, 1995.
2. Razvi, M. A. N., Chu, X. Z., Alheit, R., Werth, G., and Blümel, R., Phys. Rev. A **58**, R34–R37 (1998).
3. Dehmelt, H., Adv. At. Mol. Phys. **3**, 53–72 (1967).
4. Landau, L. D., and Lifshitz, E. M., *Mechanics*, Oxford: Pergamon Press, 1960.
5. Bahr, R. E., *Untersuchung der Eigenschaften eines Hochrequenz-Ionen-Speichers*, Freiburg: Diplom thesis, 1969.
6. Behre, E., *Bau und Erprobung einer massenselektiven Speicherionenquelle*, Freiburg: Zulassungsarbeit, 1972.
7. Peik, E., and Fletcher, J., J. Appl. Phys. **82**, 5283–5286 (1997).
8. Blümel, R., Appl. Phys. B **60**, 119–122 (1995).
9. Blümel, R., Phys. Rev. A **51**, R30–R33 (1995).
10. Blümel, R., Physica Scripta T **59**, 126–130 (1995).
11. Blümel, R., Physica Scripta T **59**, 369–379 (1995).
12. Blümel, R., Bonneville, E., and Carmichael, A., Phys. Rev. E **57**, 1511–1518 (1998).
13. Birkl, G., Kassner, S., and Walther, H., Europhys. News **23**, 143–145 (1992).
14. Habs, D., and Grimm, R., Ann. Rev. Nucl. Part. Sci. **45**, 391–428 (1995).
15. Diedrich, F., Peik, E., Chen, J. M., Quint, W., and Walther, H., Phys. Rev. Lett. **59**, 2931–2934 (1987).
16. Wineland, D. J., Bergquist, J. C., Itano, W. M., Bollinger, J. J., and Manney, C. H., Phys. Rev. Lett. **59**, 2935–2938 (1987).
17. Steck, M., Beckert, K., Eickhoff, H., Franzke, B., Nolden, F., Reich, H., Schlitt, B., and Winkler, T., Phys. Rev. Lett. **77**, 3803–3806 (1996).
18. Blümel, R., Phys. Rev. A **51**, 620–624 (1995).
19. Primack, H., and Blümel, R., Phys. Rev. E, in press.
20. Thomson, J. J., *Die Korpuskulartheorie der Materie*, Braunschweig: Vieweg, 1908.
21. Thomson, J. J., *Elektrizität und Materie*, Braunschweig: Vieweg, 1909.
22. Primack, H., and Blümel, R., "Suppression of synchrotron radiation due to beam crystallization", Eur. Phys. J. A, in press.